

Stress-strain Relationship for Steel Fiber-reinforced Lightweight Aggregate Concrete under Uniaxial Compression

H. Dabbagh*, K. Amoozraei

Department of Civil Engineering, University of Kurdistan, Sanandaj, Iran.

Article info

Article history:

Received 14 February 2019

Received in revised form

19 June 2019

Accepted 11 September 2019

Keywords:

Lightweight concrete

Steel fiber

Compressive behavior

Stress-strain model

Abstract

The current study presents a series of tests on steel fiber-reinforced lightweight aggregate concrete (SFRLWAC) cylinders in order to develop a stress-strain model for SFRLWAC subjected to compressive monotonic loading. In this experiment, steel fiber ratios of 0, 0.5, 1, and 1.5 percent by volume of the sample were used in the mixtures. The findings show that adding steel fiber to the lightweight concrete has a slight impact on the ascending branch of the stress-strain curve; however, it has a noticeable influence on the descending branch. The peak stress, strain at peak stress, and modulus of elasticity were investigated. To this end, some equations were established. To predict the complete SFRLWAC stress-strain curve, a stress-strain model was introduced and the validity of the model was explored. There was a good agreement between the proposed model data and experimental findings. Using ABAQUS software, numerical simulation of the SFRLWAC beams subjected to monotonic loading was conducted; the simulated results had an acceptable agreement with the experimental data.

1. Introduction

Compared with normal-weight concrete, lightweight concrete has lower density. Different kinds of lightweight concrete based on the production type, including using porous lightweight aggregate, introducing the large voids within the mortar or concrete, and excluding the fine aggregate from the mixture, are defined. Moreover, given the application objective, it is divided into structural lightweight concrete, masonry-unit concrete, and insulating concrete [1]. This study also delves into structural lightweight aggregate concrete (LWAC). According to ACI 318, the compressive strength of cylinders in a 28-day time interval must be over 17MPa, and the maximum point for density must be 1840kg/m³ for LWAC [2].

Adequate thermal insulation, appropriate durability, dead-load decline, and preferable fire resistance,

are instances of LWAC advantages [3, 4]. Hence, thanks to its suitable characteristics, LWAC was employed for structural purposes [5-8]. However, factors including brittleness and low strength, limit the extensive structural application of LWAC [9-11]. On the other hand, adding steel fibers, as a ductile material, enhances many characteristics of concrete such as flexural and tensile strength and toughness [12-16].

The impact of steel fiber on the characteristics of concrete will be controlled by the fiber material, fiber aspect ratio (ld), and fiber content (V_f) [17]. The impact of V_f and ld on the workability and mechanical properties of concrete has been reported in the literature [18-21].

In addition, steel fiber is capable to alter the structural performance of LWAC. In order to model and stimulate the reaction of a structure under various conditions, statistical data of the material behavior should

*Corresponding author: H. Dabbagh (Assistant Professor)

E-mail address: h.dabbagh@uok.ac.ir

<http://dx.doi.org/10.22084/jrstan.2019.18088.1077>

ISSN: 2588-2597

be available. Therefore, for an efficient prediction of the structural response, one must determine the impact of materials that are used on the behavior of concrete members. Besides, the significance of studying the compressive stress-strain curve of concrete should not be overlooked [22-24]. Some studies have been conducted on the compressive behavior of steel fiber-reinforced concrete [25-28]. Despite some proposed models for steel fiber-reinforced concrete, none are capable of precise prediction of compressive response of steel fiber-reinforced lightweight concrete. Therefore, proposing a new model for SFRLWAC is of major importance.

At the first stage of a step-by-step research, authors investigated the impact of steel fiber content on the compressive behavior of SFRLWAC [29]. In the current paper, as the second stage of the main research, the primary aim as well as the novelty of the research is linked to proposing a stress-strain model for steel fiber-reinforced lightweight aggregate concrete.

2. Experimental Program

In order to determine the impact of steel fiber on the stress-strain curve and the behavior of LWAC, an experimental plan was designed and the uniaxial compressive test was carried out. The exhaustive specifications of the experimental plan are as follows.

2.1. Materials and Mix Proportions

In providing the specimens, the scoria aggregate (maximum size, 12.5mm) was used as fine and coarse lightweight aggregate. The fine and coarse aggregates showed water absorption of 16% and 12%, respectively. The used cement was ordinary Portland cement (Type

I). The aggregate grading was conducted according to ASTM C330 [30].

As it is illustrated in Fig. 1, two types of steel fibers used in this study were straight hooked-end (SF₁) and crimped (SF₂). Steel fibers with contributing content of 30% crimped and 70% straight hooked-end fiber were added to the mix to make the optimum mix design [31]. For the mixes that consisted of steel fiber, fiber contents of 0.5%, 1%, and 1.5% were used. Furthermore, to obtain a better practical level in terms of workability, a Polycarboxylic ether-based superplasticizer was added to the mixtures. Table 1 indicates further information on the employed materials. To design the concrete mix, the volumetric method, ACI 211.2 [32] was used. Table 2 presents the structure and characteristics of the mixtures.

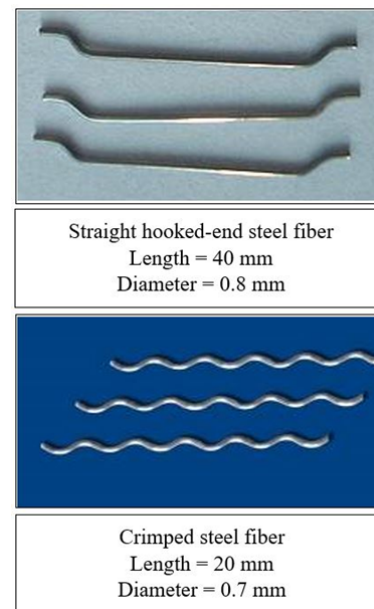


Fig. 1. Steel fibers used in this study.

Table 1
Material properties.

Materials	Type	Specific density (kg/m ³)
Cement	Ordinary portland (Type I)	3150
Fine lightweight aggregate	Scoria	Bulk density: 772 Apparent specific gravity: 1650
Coarse lightweight aggregate	Scoria	Bulk density: 680 Apparent specific gravity: 1530
Superplasticizer	Polycarboxylic ether	1080
Steel fiber (SF)	Straight-hooked end steel fiber	7800

Table 2
Mix proportions.

Samples	C (kg/m ³)	CA (kg/m ³)	FA (kg/m ³)	W/C Ratio	SP (kg/m ³)	SF (Vol %)
F00 (Ref)	460	528	584	0.31	2.4	-
F05 (0.5% fiber)	460	528	584	0.31	2.5	0.5
F10 (1% fiber)	460	528	584	0.31	2.6	1.0
F15 (1.5% fiber)	460	528	584	0.31	2.7	1.5

C: Cement, CA: Coarse aggregate, FA: Fine aggregate, W: Water, SP: Super plasticizer, SF: Steel fiber

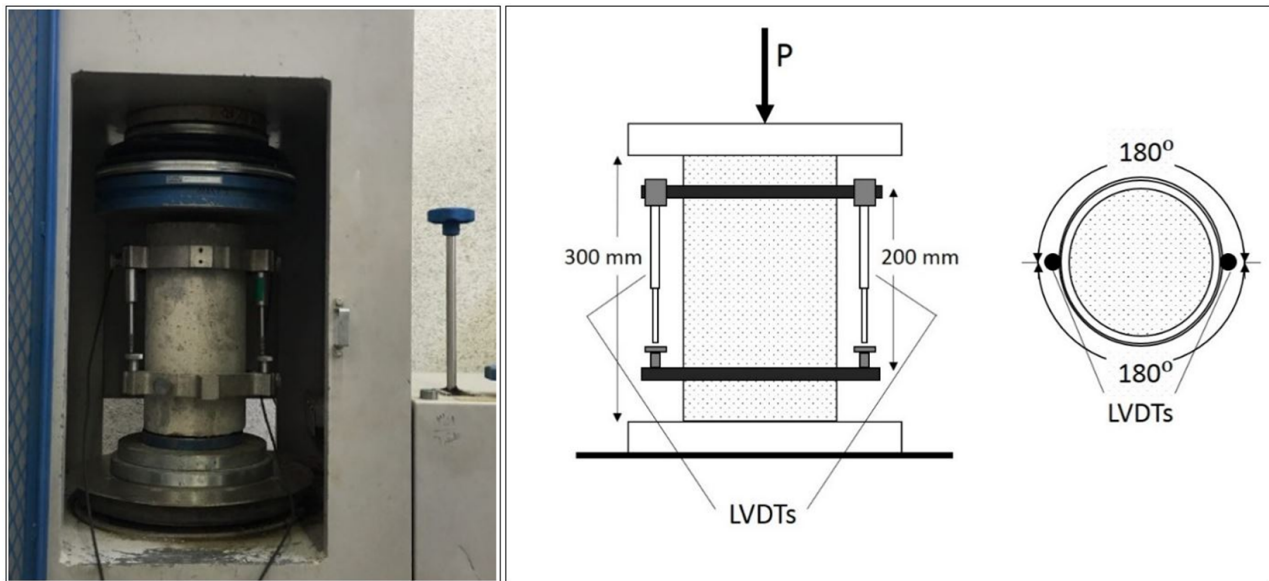


Fig. 2. Test setup for generating stress-strain curve.

2.2. Test Specimens, Mixing, Casting, and Curing

In the present study, four mixes were prepared that contained 0%, 0.5%, 1%, and 1.5% steel fiber ratios by volume of the sample.

Initially, fine lightweight aggregate was blended with coarse lightweight aggregate. Then, some other materials, including water with superplasticizer, steel fibers, and cement were added to the mixtures. Subsequent to the mixing process, the mixed compositions were cast into the molds and vibrated with shaking table. To prevent the humidity loss, the polyethylene sheets were utilized to cover the cylinders' surface. After 24 hours, the specimens were demolded and cured over 28 days in water at $23 \pm 2^\circ\text{C}$. In order to achieve a smooth surface for the uniformed transfer of the load, the cylindrical specimens were capped with sulfur capping compound before testing. Three $150 \times 300\text{mm}$ cylinders were tested for each mix to accomplish the monotonic stress-strain curve; the average of which is shown as the result of the test.

2.3. Test Procedure and Setup

The schematic design of the test set-up is illustrated in Fig. 2. In order to discover the monotonic curves, a 3000kN hydraulic compressive testing machine was employed for testing the specimens. Hydraulic jacks with 50mm maximum ram travel, a bottom platen, and a load spreader, formed the loading assembly. ASTM C469 [33] was used to investigate the modulus of elasticity whereas compressive strength was examined using ASTM C39 [34]. In order to plot the stress-strain curves, the displacement was measured by two linear variable differential transducers (LVDTs); they were set parallel to the loading direction. Moreover, a cir-

cular steel frame was made to grip the LVDTs. The axial deformation of the cylinders was monitored by the LVDTs and was captured using a data logger. The output of the data logger was averaged for more accurate results.

In this investigation, the middle two-thirds of the height of the cylindrical specimens were considered to calculate the deformation of samples in order to avoid end effects. With the progress of the loading, the uniaxial load continued to be concentric to the specimens.

3. Experimental Results

Steel fiber-reinforced lightweight concrete was subjected to the compressive monotonic loading. The stress-strain curve was achieved and the compressive behavior of SFRLWAC was probed. Strain at peak stress (ε_0), modulus of elasticity (E), and the compressive strength (f_c), that are among the most important parameters of the stress-strain curve, were all delineated. Applying regression analysis gave the equations for defining these parameters. In addition, the effect of fiber on the failure mode was also studied.

3.1. Monotonic Stress-strain Curve

According to Fig. 3, for the monotonic curve of all specimens, the linear elastic part of the ascending branch extends up to approximately 80% of the peak stress. The findings indicate that steel fibers have a minor influence on the ascending part and the significant values on the monotonic curve, i.e., f_c , E , and ε_0 have a slight increase (Table 3). However, the impact on the descending branch is considerable. Monotonic Curve of SFRLWAC was explored in details by authors in another paper [29].

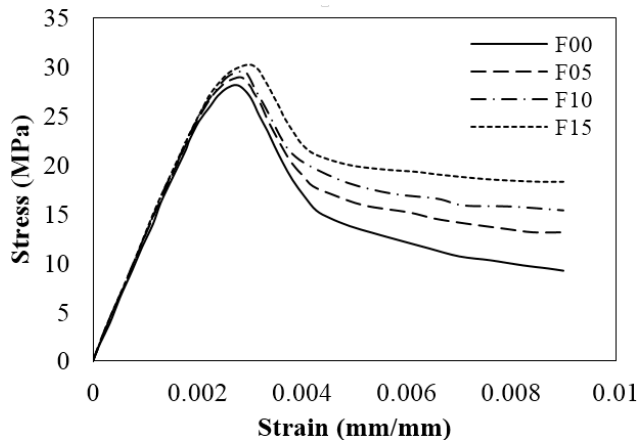


Fig. 3. Compressive stress-strain curve of SFRLWAC [29].

3.2. Compressive Strength

As it is illustrated in Fig. 4, the compressive strength of SFRLWAC at various volume portions was determined. The compressive strength of SFRLWAC is associated with the fiber volume fraction. Applying regression analysis gives the following equation:

$$f_c = 134V_f + f'_c, \quad R^2 = 0.99 \quad (1)$$

where f_c is compressive strength of SFRLWAC in MPa, f'_c is compressive strength of plain lightweight concrete in MPa, and V_f is steel fiber volume fraction.

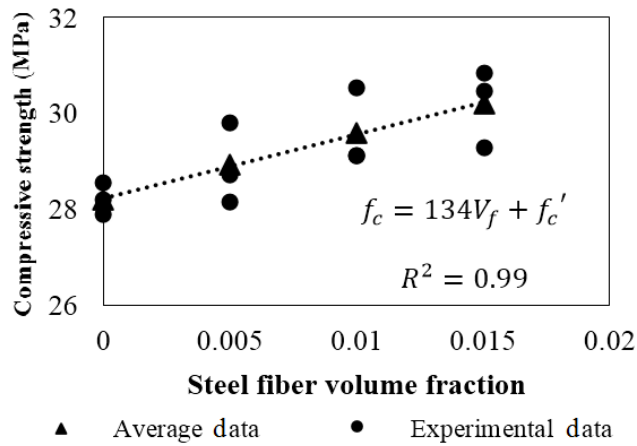


Fig. 4. Relationship between f_c and V_f .

3.3. Strain at Peak Stress

The strain at peak stress versus the respective f_c for each specimen, is presented in Fig. 5. The results show that by adding steel fiber, ϵ_0 increases which is presented in Table 3. By applying regression analysis, the following expression for ϵ_0 is derived:

$$\epsilon_0 = 11.78 \times 10^{-5} f_c - 0.00058 \quad (2)$$

$$R^2 = 0.99$$

where ϵ_0 is strain at peak stress in mm/mm.

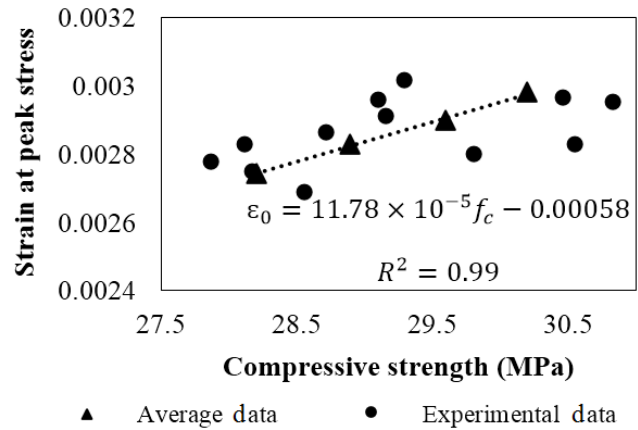


Fig. 5. Relationship between ϵ_0 and f_c .

3.4. Modulus of Elasticity

For samples containing 0, 0.5, 1, and 1.5 percent steel fiber, modulus of elasticity is 12.18, 12.32, 12.48, and 12.67GPa, respectively. Results show that adding steel fiber does not have a noticeable impact on the modulus of elasticity. In comparison with F00, E upgrades 1.15%, 2.5%, and 4% for specimens containing 0.5%, 1%, and 1.5% steel fiber, respectively. The trivial effect of steel fiber on the enhancement of E has been considered in the past research [35]. According to the experimental findings, the following relationship for E of SFRLWAC is established (Fig. 6).

$$E = 2.296\sqrt{f_c}, \quad R^2 = 0.97 \quad (3)$$

where E is modulus of elasticity in GPa.

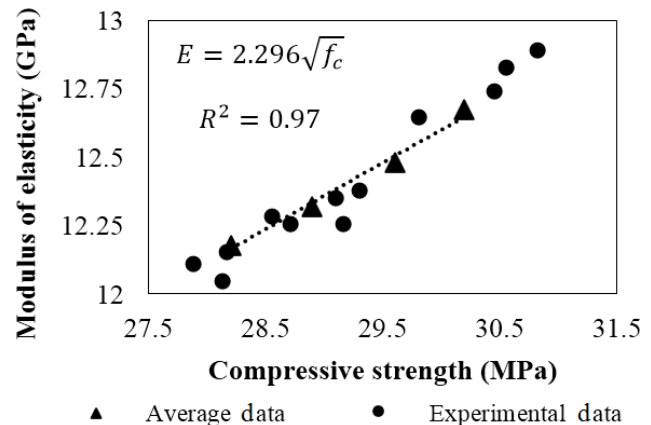


Fig. 6. Relationship between E and f_c .

3.5. Failure Mode

The response of the cylindrical specimens at or near the peak load affects f_c and ϵ_0 . At the peak load level, cracks will be created in the cylindrical specimens in consequence of lateral expansion in LWAC. Fig. 7 shows the failure mode of LWAC containing different volume fractions of steel fiber after testing.

Table 3
Experimental results.

Samples	No.	f_c (MPa)		E (GPa)		ε_0 (mm/mm)	
		Specimen	Average	Specimen	Average	Specimen	Average
F00	1	28.55		12.28		0.00269	
	2	27.88	28.2	12.11	12.18	0.00278	0.00274
	3	28.17		12.15		0.00275	
F05	1	28.72		12.26	12.32	0.00286	
	2	29.80	28.9	12.65		0.00280	0.00283
	3	28.12		12.05		0.00283	
F10	1	29.10		12.35		0.00296	
	2	30.55	29.6	12.83	12.48	0.00283	0.00290
	3	29.15		12.26		0.00291	
F15	1	29.30		12.38	12.67	0.00302	
	2	30.82	30.2	12.89		0.00295	0.00298
	3	30.45		12.74		0.00297	

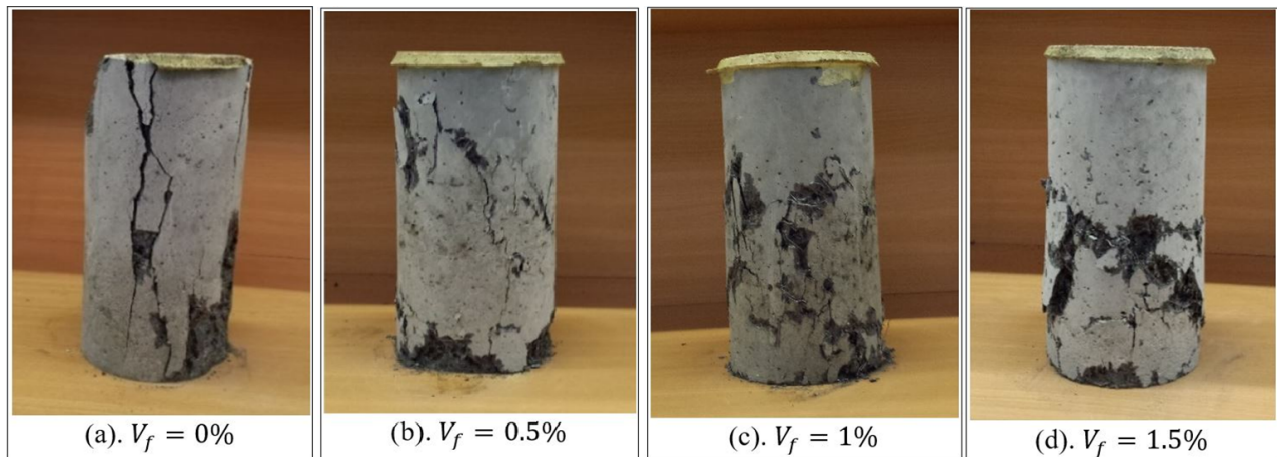


Fig. 7. Failure mode of SFRLWAC.

The crack propagation in the plain lightweight concrete is parallel to the loading direction (Fig. 7a); raising the steel fiber content, the cracks bend slowly and change perpendicularly to the loading direction (Figs. 7b, c, and d). Convexity in the lateral direction with the formation of the cracks along the outer surface and adjacent to the middle belt of cylindrical specimens is noticeable in this type of failure. The regular failure surface is established in plain concrete. However, the failure surface of SFRLWAC is unstable. Steel fibers contribute to keeping the concrete matrix together by bridging across the cracks and limiting the crack propagation.

4. Proposed Equation (Stress-strain Model)

To propose an expression for stress-strain curve of concrete, the conditions, including the concordance between the proposed model and experimental findings, defining both ascending and descending branches of

the monotonic curve, the simplicity of the equation, and the establishment of the model based on the physically important parameters, f_c , ε_0 , and E , should be considered. These parameters can be delimited by the experimental findings [36].

A number of studies have been conducted to propose a stress-strain model for concrete. Some of the most important empirical stress-strain models accessible in the literature were investigated and the empirical equation established by Popovics [22] was employed as a basis to study an equation suitable for the SFRLWAC due to its plainness and exactness. Popovics's model was established for normal-weight concrete; in addition, it could not indicate the influence of steel fiber on the stress-strain curve. The following can be introduced for the stress-strain model of the compressive stress-strain curve of SFRLWAC:

$$\frac{\sigma}{f_c} = \frac{\beta \left(\frac{\varepsilon}{\varepsilon_0} \right)}{\beta - 1 + \left(\frac{\varepsilon}{\varepsilon_0} \right)^\alpha} \quad (4)$$

$$\alpha = \beta = 6 - 32(V_f)^{0.66}, \quad \varepsilon \leq \varepsilon_0 \quad (5)$$

$$\alpha = 1.6 - 70V_f, \quad \varepsilon > \varepsilon_0 \quad (6)$$

$$\beta = 0.6 - 25V_f, \quad \varepsilon > \varepsilon_0 \quad (7)$$

where σ and ε are the stress and strain values on the curve, respectively and α and β are the material parameters dependent on the stress-strain curve shape.

Based on the experimental findings, the best fitting statistical analysis was conducted to establish a relationship between the material parameters α and β regarding V_f .

5. Fit of the Experimental Findings and Empirical Equation

Figs. 8 (a-d) show the stress-strain curve of SFRLWAC obtained by the proposed model and the experimental tests. Fit of the predicted curve and the experimental test result curve demonstrates a good agreement at different steel fiber volume fractions. The experimental finding and the suggested equation for the ascending branch of the stress-strain curve indicate a remarkable congruity. The suggested equation displays the

insignificant influence of steel fiber on the developing E and f_c of LWAC. The model explains that by adding more steel fibers, the ascending branch of the monotonic curve has a slight transformation, which accords with the experimental findings. The formed curve for the descending part by the model shows that employing steel fiber ends in drop-decrease of strength after the peak stress, which contributes to an adequate fit with the test results. Thus, the established model can be useful to predict the behavior of SFRLWAC by producing the stress-strain curve.

The uniaxial monotonic tests of Libre et al. [37] and Campione et al. [38] were considered and the experimental findings were compared with the results obtained by the proposed model. Libre et al. used pumice stone as coarse aggregate and the river sand as fine aggregate. The samples of their study contained 0%, 0.5%, and 1% hooked-end steel fiber. Campione et al. utilized pumice and river sand as coarse and fine aggregate, respectively. Furthermore, in their study, 0%, 0.5%, 1%, and 2% hooked-end steel fibers were used. Fig. 9 shows the experimental test results compared with the proposed model. The findings indicate a notable correspondence between laboratory test results and the suggested model for the descending and ascending branches of the stress-strain curve.

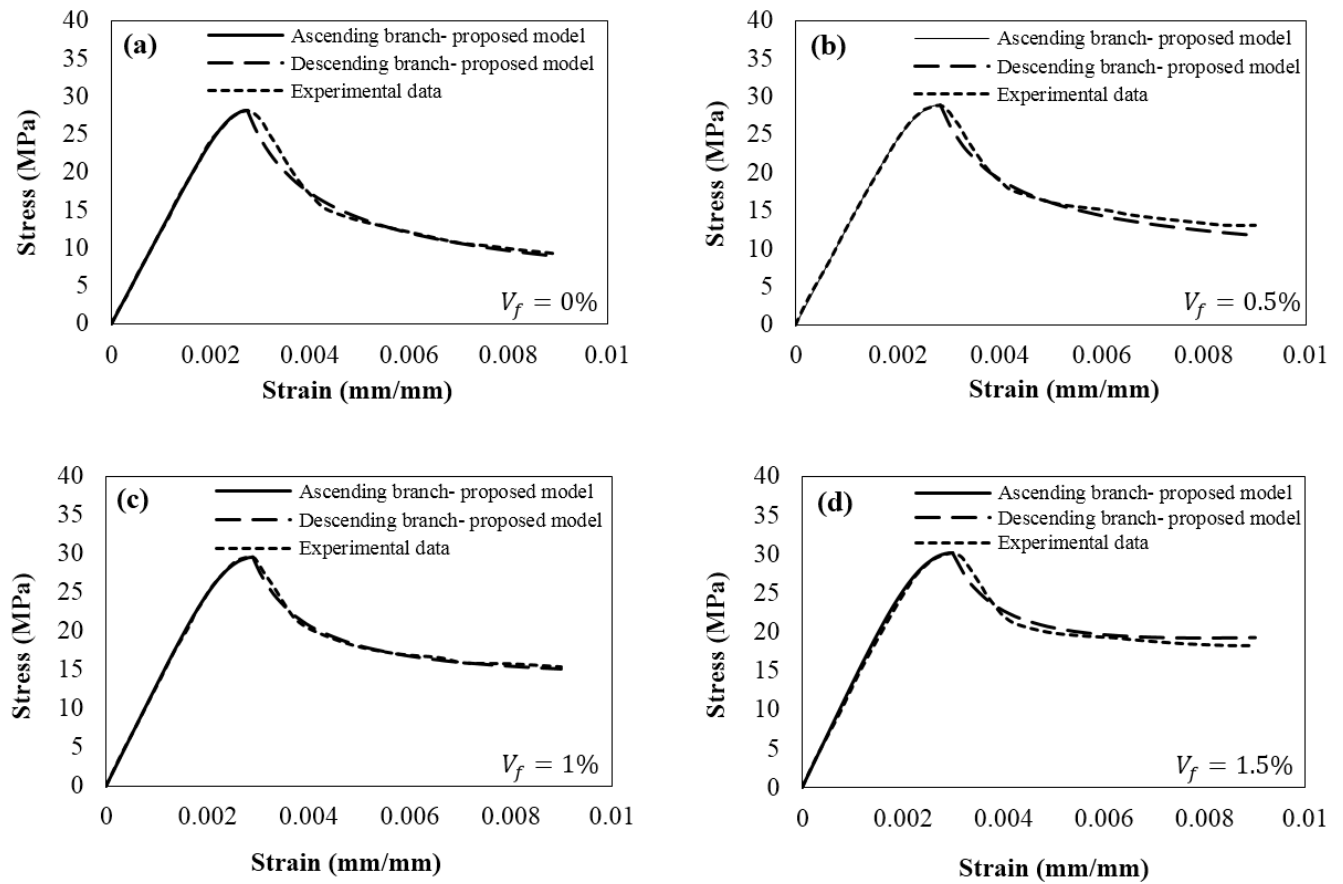


Fig. 8. Experimental versus proposed model result.

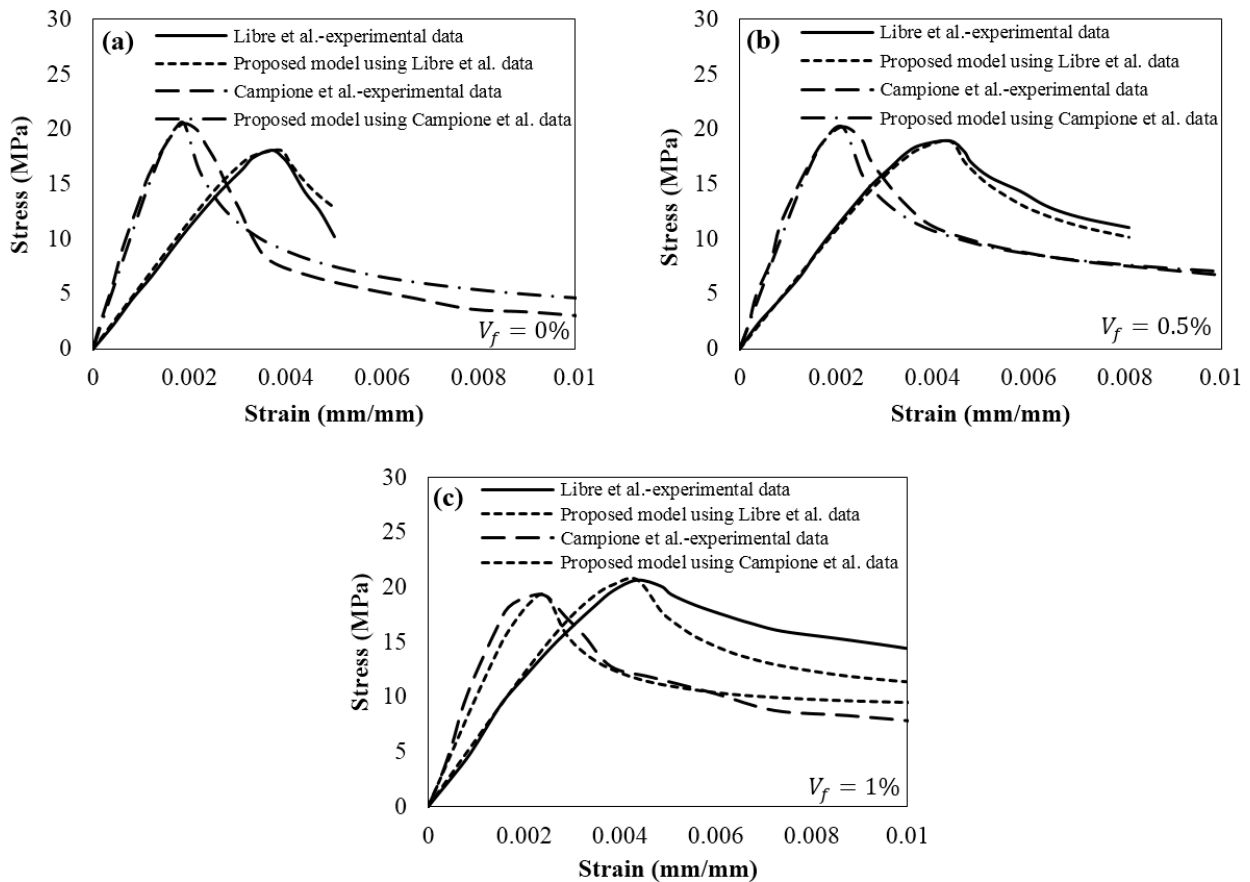


Fig. 9. Comparison between experimental results of other studies and the proposed model [37, 38].

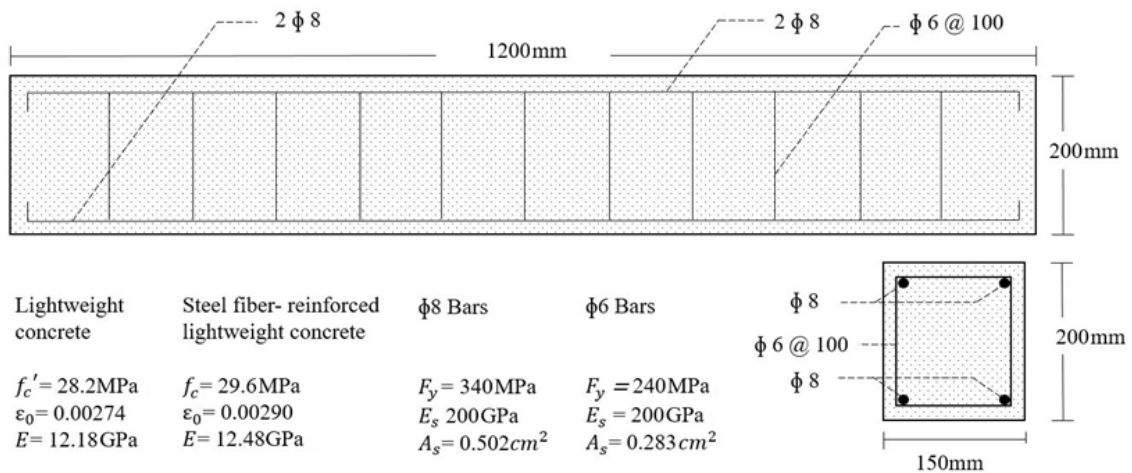


Fig. 10. Details of beam and material properties [39].

6. Analysis of Beam

To get an initial proof of the fittingness of the proposed approach to the monotonic response modeling of steel fiber-reinforced lightweight aggregate concrete, an analysis of beams was undertaken. The experimental data for lightweight concrete and steel fiber-reinforced lightweight concrete beam subjected to the monotonic loading when the point load acts uniformly at the mid-span came from literature [39].

In this experimental program, reinforced LWAC beams of 200×150mm rectangular cross section and 1200 mm overall length were fabricated. No. 8 deformed bar and No. 6 bar were used for longitudinal and transverse reinforcements, respectively. The minimum amount of steel bar reinforcement was considered for all beam specimens (ACI 318, 2011) to accurately assess the effects of steel fibers used in the LWAC mixes. The value of longitudinal reinforcement ratio was 0.72% for specimens.

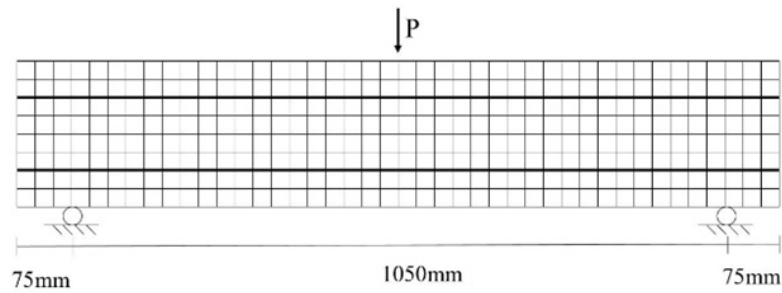


Fig. 11. Finite element mesh used to model beam.

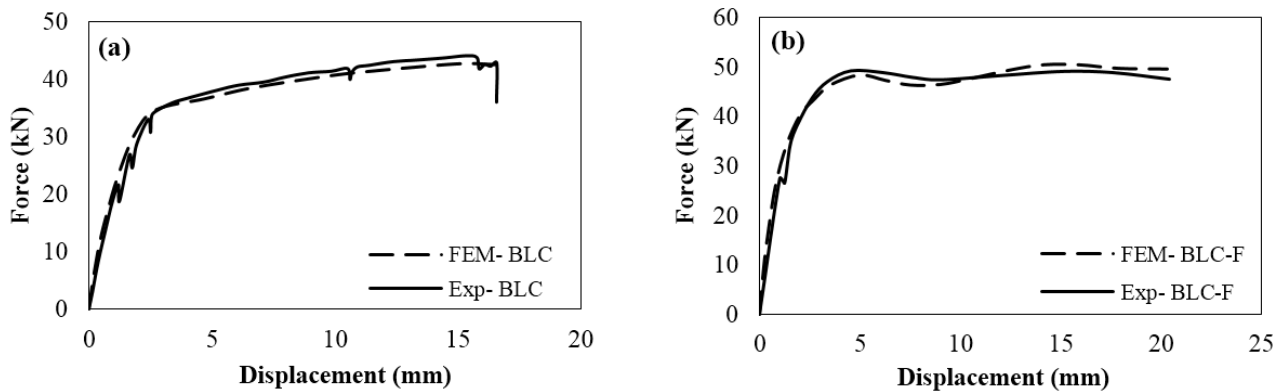


Fig. 12. Response of Beam: Experimentally measured response versus predicted response.

Two types of beams were prepared: lightweight aggregate concrete beam (BLC, as reference), and steel fiber-reinforced lightweight aggregate concrete beam (BLC-F, containing 1% steel fiber). Reinforcement details and material properties are given in Fig. 10.

Beam BLC and BLC-F were modeled in ABAQUS using the finite element mesh shown in Fig. 11. 8-node cubic mesh and 2-node mesh was applied to model the beam and bars, respectively; Wire model was used for bars. It should be noted that mesh size of all elements was 25mm. Concrete damaged plasticity model was employed for the analysis of concrete materials. Besides, the established stress-strain model, Eqs. (4-7), was applied in ABAQUS software in order to simulate beams.

The load-displacement data from experimental test and finite element method analysis of reference and steel fiber-reinforced lightweight beam is illustrated in Fig. 12. The comparison between the experimental findings and finite element analysis data in linear and nonlinear region indicates an acceptable agreement.

7. Conclusions

Based on the present experimental research, the following conclusions can be derived:

1. Steel fiber addition has an insignificant impact on the ascending branch of the monotonic curve in LWAC; which results in a slight increase in the compressive strength, the strain relevant to

the maximum stress, and the modulus of elasticity. Steel fibers have a significant impact on the descending part of the stress-strain curve. Moreover, the reduction rate in strength beyond the maximum stress drops, which is caused by the ductility and energy absorption of fiber.

2. Employing data fitting process resulted in establishing a relationship between the steel fiber volume fraction and the compressive strength. Moreover, after the regression analysis, what was derived was the expressions for the strain at peak stress and modulus of elasticity regarding the compressive strength.
3. Adding steel fibers results in changes in the direction of crack propagation. For plain lightweight concrete, the cracks propagate parallel to the loading direction. Yet, in steel fiber-reinforced lightweight concrete, the cracks slowly incline, becoming perpendicular to the loading direction.
4. In order to predict the ascending and descending branches of the stress-strain curve of steel fiber-reinforced lightweight aggregate concrete, a stress-strain model was suggested. The comparative study shows a proper agreement between the experimental test results and the proposed stress-strain curve.
5. Steel fiber-reinforced lightweight concrete beams subjected to monotonic loading were modeled in

ABAQUS software. The results showed an acceptable agreement between the simulated and experimental results.

Acknowledgements

We express our gratitude to the Concrete Research Laboratory, University of Kurdistan, Iran, for their cooperation.

References

- [1] A.M. Neville, J.J. Brooks, Concrete technology, Harlow, Essex UK: Longman Scientific & Technical, New York, John Wiley, (1987).
- [2] ACI Committee, Building code requirements for structural concrete (ACI 318-05) and commentary (ACI 318R-05). American Concrete Institute, (2005).
- [3] C.L. Hwang, M.F. Hung, Durability design and performance of self-consolidating lightweight concrete, *Const. Build. Mater.*, 19(8) (2005) 619-626.
- [4] A. Bilodeau, V.K.R. Kodur, G.C. Hoff, Optimization of the type and amount of polypropylene fibres for preventing the spalling of lightweight concrete subjected to hydrocarbon fire, *Cem. Concr. Compos.*, 26(2) (2004) 163-174.
- [5] K. Melby, E.A. Jordet, C. Hansvold, Long-span bridges in Norway constructed in high-strength LWA concrete, *Eng. Struct.*, 18(11) (1996) 845-849.
- [6] A.K. Haug, S. Fjeld, A floating concrete platform hull made of lightweight aggregate concrete, *Eng. Struct.*, 18(11) (1996) 831-836.
- [7] J.A. Rossignolo, M.V. Agnesini, J.A. Morais, Properties of high-performance LWAC for precast structures with Brazilian lightweight aggregates, *Cem. Concr. Compos.*, 25(1) (2003) 77-82.
- [8] E. Yasar, C.D. Atis, A. Kilic, H. Gulsen, Strength properties of lightweight concrete made with basaltic pumice and fly ash, *Mater. Lett.*, 57(15) (2003) 2267-2270.
- [9] M.N. Haque, H. Al-Khaiat, O. Kayali, Strength and durability of lightweight concrete, *Cem. Concr. Compos.*, 26(4) (2004) 307-314.
- [10] M.H. Zhang, O.E. Gjvorv, Mechanical properties of high-strength lightweight concrete, *ACI Mater. J.*, 88(3) (1991) 240-247.
- [11] T.P. Chang, M.M. Shieh, Fracture properties of lightweight concrete, *Cem. Concr. Res.*, 26(2) (1996) 181-188.
- [12] G. Campione, N. Miraglia, M. Papia, Mechanical properties of steel fibre reinforced lightweight concrete with pumice stone or expanded clay aggregates, *Mater. Struct.*, 34(4) (2001) 201-210.
- [13] T. Uygunoğlu, Investigation of microstructure and flexural behavior of steel-fiber reinforced concrete, *Mater. Struct.*, 41(8) (2008) 1441-1449.
- [14] M. Hassanpour, P. Shafigh, H.B. Mahmud, Lightweight aggregate concrete fiber reinforcement—a review, *Const. Build. Mater.*, 37 (2012) 452-461.
- [15] Y. Hao, H. Hao, G. Chen, Experimental investigation of the behaviour of spiral steel fibre reinforced concrete beams subjected to drop-weight impact loads, *Mater. Struct.*, 49(1-2) (2016) 353-370.
- [16] K.H. Mo, S.H. Goh, U.J. Alengaram, P. Visintin, M.Z. Jumaat, Mechanical, toughness, bond and durability-related properties of lightweight concrete reinforced with steel fibres, *Mater. Struct.*, 50(1) (2017) 46.
- [17] P. Suraneni, P.C.B. Anleu, R.J. Flatt, Factors affecting the strength of structural lightweight aggregate concrete with and without fibers in the 1,200-1,600kg/m³ density range, *Mater. Struct.*, 49(1-2) (2016) 677-688.
- [18] A. Bentur, S. Mindess, Fibre reinforced cementitious composites, CRC Press, (2014).
- [19] P. Pierre, R. Pleau, M. Pigeon, Mechanical properties of steel microfiber reinforced cement pastes and mortars, *J. Mater. Civ. Eng.*, 11(4) (1999) 317-324.
- [20] W. Abbass, M.I. Khan, S. Mourad, Evaluation of mechanical properties of steel fiber reinforced concrete with different strengths of concrete, *Const. Build. Mater.*, 168 (2018) 556-569.
- [21] J. Thomas, A. Ramaswamy, Mechanical properties of steel fiber-reinforced concrete, *J. Mater. Civ. Eng.*, 19(5) (2007) 385-392.
- [22] S. Popovics, A numerical approach to the complete stress-strain curve of concrete, *Cem. Concr. Res.*, 3(5) (1973) 583-599.
- [23] P. Kumar, A compact analytical material model for unconfined concrete under uni-axial compression, *Mater. Struct.*, 37(9) (2004) 585-590.
- [24] A.A. Tasnimi, Mathematical model for complete stress-strain curve prediction of normal, lightweight and high-strength concretes, *Mag. Concr. Res.*, 56(1) (2004) 23-34.

- [25] M.C. Nataraja, N. Dhang, A.P. Gupta, Stress-strain curves for steel-fiber reinforced concrete under compression, *Cem. Concr. Compos.*, 21(5-6) (1999) 383-390.
- [26] J.A.O. Barros, J.A. Figueiras, Flexural behavior of SFRC: testing and modeling, *J. Mater. Civ. Eng.*, 11(4) (1999) 331-339.
- [27] A.S. Ezeldin, P.N. Balaguru, Normal-and high-strength fiber-reinforced concrete under compression, *J. Mater. Civ. Eng.*, 4(4) (1992) 415-429.
- [28] P. Soroushian, C.D. Lee, Constitutive modeling of steel fiber reinforced concrete under direct tension and compression, In: R.N. Swamy, B. Barr, editors, *Fiber reinforced cement and concrete recent developments*, Cardiff, UK: University of Wales; Publication of: Elsevier Applied Science Publishers Limited, 18(20) (1989) 363-377.
- [29] H. Dabbagh, K. Amoorezaei, S. Akbarpour, K. Babamuradi, Compressive toughness of lightweight aggregate concrete containing different types of steel fiber under monotonic loading, *AUT. J. Civ. Eng.*, 1(1) (2017) 15-22.
- [30] ASTM C330/C330M, Standard specification for lightweight aggregates for structural concrete, American Society for Testing and Materials, (2014).
- [31] K. Amoorezaei, Behavior of steel fiber reinforced lightweight aggregate concrete under compressive cyclic loading, MSc Thesis, Iran: University of Kurdistan, (2016).
- [32] ACI 211.2, Standard practice for selecting proportions for structural lightweight concrete, American Concrete Institute, 1998 (Reapproved 2004).
- [33] ASTM C469/C469M, Standard test method for static modulus of elasticity and Poisson's ratio of concrete in compression, American Society for Testing and Materials, (2014).
- [34] ASTM C39/C39M, Standard test method for compressive strength of cylindrical concrete specimens, American Society for Testing and Materials, (2015).
- [35] P. Mehta, P.J.M. Monteiro, *Concrete: microstructure, properties, and materials*, McGraw-Hill Publishing, (2006).
- [36] D.J. Carreira, K.H. Chu, Stress-strain relationship for plain concrete in compression, *ACI J. Proc.*, 82(6) (1985) 797-804.
- [37] N.A. Libre, M. Shekarchi, M. Mahoutian, P. Soroushian, Mechanical properties of hybrid fiber reinforced lightweight aggregate concrete made with natural pumice, *Const. Build. Mater.*, 25(5) (2011) 2458-2464.
- [38] G. Campione, L. La Mendola, Behavior in compression of lightweight fiber reinforced concrete confined with transverse steel reinforcement, *Cem. Concr. Compos.*, 26(6) (2004) 645-656.
- [39] S. Akbarpour, The effects of nano-silica and steel fibers on flexural behavior of reinforced lightweight aggregate concrete beams, PhD Thesis, Iran: University of Kurdistan, (2018).